

The influence of pd mixing and magnetic interactions on the pre-edge peak intensity at the Co (Ni) K absorption edge in $\text{Co(Ni)}_c\text{Mg}_{1-c}\text{O}$ solid solutions

A Kuzmin[†], N Mironova[‡] and J Purans[†]

[†] Institute of Solid State Physics, 8 Kengaraga Street, LV-1063 Riga, Latvia

[‡] Nuclear Research Centre, Latvian Academy of Science, LV-2169 Salaspils, Latvia

Received 15 January 1997, in final form 3 March 1997

Abstract. In this work, the variation of the pre-edge peak at the Co (Ni) K absorption edge in $\text{Me}_c\text{Mg}_{1-c}\text{O}$ ($\text{Me} = \text{Co}, \text{Ni}$) solid solutions is studied upon dilution. Its intensity is attributed to the number of $|3d^{n+i}\underline{L}^i\rangle$ ($i > 0$) ground-state configurations with oxygen 2p hole(s) denoted by \underline{L}^i . Upon dilution, the pre-edge peak intensity grows by about a factor of 1.2 in $\text{Ni}_c\text{Mg}_{1-c}\text{O}$ and about a factor of 2.8 in $\text{Co}_c\text{Mg}_{1-c}\text{O}$. This fact is explained by an increase of the 2p(O)–3d(Me) mixing. The results obtained are in agreement with the modifications of the local atomic structure around Co^{2+} and Ni^{2+} ions, probed by extended x-ray absorption fine structure (EXAFS), and optical spectroscopies. The correlation between the concentration dependences of the pre-edge peak intensity and the Néel temperature for solid solutions is also discussed.

1. Introduction

The CoO-MgO and NiO-MgO solid solutions belong to a class of the diluted face-centred-cubic (fcc) antiferromagnets whose magnetic and related properties have been intensively studied during the last fifteen years [1–11]. The established magnetic phase diagrams of $\text{Co}_c\text{Mg}_{1-c}\text{O}$ [2, 3, 11] and $\text{Ni}_c\text{Mg}_{1-c}\text{O}$ [6, 7] were found to be rather similar: they suggest a single phase transition upon cooling from a paramagnetic-like to an antiferromagnetic-like state for all concentrations c above the percolation threshold c_p ($c_p \simeq 0.2$ [6] ($c_p \simeq 0.15$ [7]) for $\text{Ni}_c\text{Mg}_{1-c}\text{O}$ and $c_p \simeq 0.13$ [2, 3] for $\text{Co}_c\text{Mg}_{1-c}\text{O}$).

Pure CoO and NiO belong to the group of type-II antiferromagnetic (AF_2) charge-transfer insulators [12, 13] with the Néel temperatures $T_N = 289$ and 523 K [14], respectively. The magnetic interactions in the fcc antiferromagnets are characterized by the relative signs and strengths of the nearest-neighbour (NN), J_{NN} , and the next-nearest-neighbour (NNN), J_{NNN} , superexchange interactions between two transition metal (TM) ions via an oxygen ion [15]. The NN interactions, having ferromagnetic and antiferromagnetic character, occur within three-atom chains, $\text{Ni}^{2+}-\text{O}^{2-}-\text{Ni}^{2+}$, with $\widehat{\text{NiONi}} = 90^\circ$ (the so-called 90° pairs), while the NNN interactions, having antiferromagnetic character, occur within linear three-atom chains, $\text{Ni}^{2+}-\text{O}^{2-}-\text{Ni}^{2+}$, with $\widehat{\text{NiONi}} = 180^\circ$ (the so-called 180° pairs). The values of J_{NN} and J_{NNN} for CoO are, respectively, 5.5 and 27.4 K, while for NiO they are, respectively, $\simeq 34$ and 202 K [3, 7]. The larger strengths of the superexchange interactions, J_{NN} and J_{NNN} , for NiO , compared to those for CoO , explain why nickel oxide has a Néel temperature T_N higher than that of cobalt oxide.

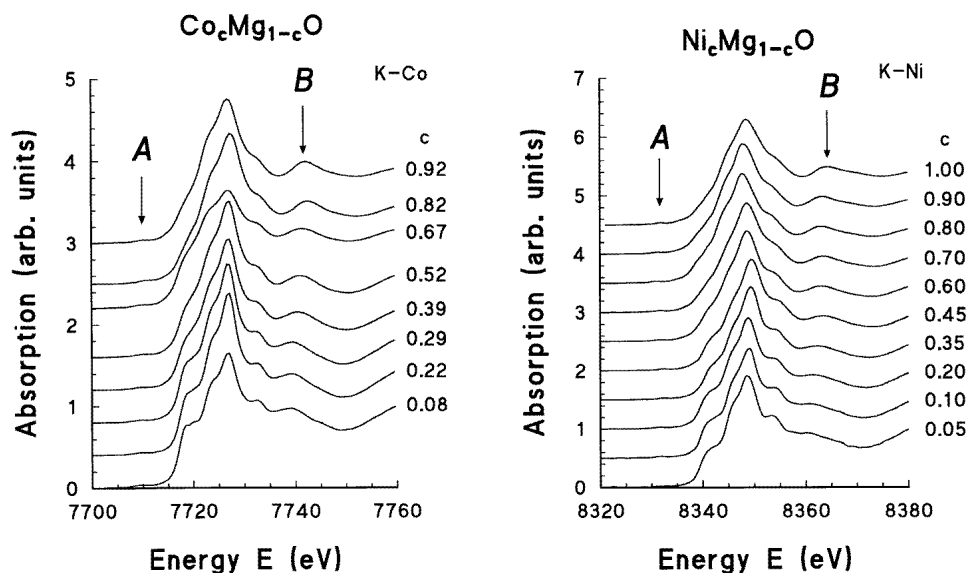


Figure 1. Normalized x-ray absorption near-edge structure (XANES) at the Ni and Co K edges in $\text{Ni}_c\text{Mg}_{1-c}\text{O}$ and $\text{Co}_c\text{Mg}_{1-c}\text{O}$ solid solutions. The positions of the pre-edge peak A and the feature B are indicated by arrows.

It is important that both J_{NN} - and J_{NNN} -interactions are of short range, and, therefore, should be influenced by the variation of the local environment around the magnetic ions. According to the x-ray diffraction (XRD) [2, 7], the lattice parameter a in solid solutions depends linearly on the composition. Upon dilution, it decreases from $a = 4.2615 \text{ \AA}$ in CoO , and increases from $a = 4.1795 \text{ \AA}$ in NiO to the value 4.2113 \AA in pure MgO ; thus, the maximum variation of a is about 1.1% in $\text{Co}_c\text{Mg}_{1-c}\text{O}$ and about 0.8% in $\text{Ni}_c\text{Mg}_{1-c}\text{O}$. Therefore, since the crystal structure of $\text{Me}_c\text{Mg}_{1-c}\text{O}$ ($\text{Me} = \text{Co}, \text{Ni}$) does not change upon dilution, and also the variation of the lattice parameter a is small, it is expected that J_{NN} and J_{NNN} should be not significantly affected by dilution [7]. Under this assumption, the Néel temperature of solid solutions depends, within the mean-field theory [16], only on the number of next-nearest-neighbour TM ions which are involved in the 180° superexchange interaction.

However, the XRD, being sensitive to the long-range order (LRO), provides us only with averaged information on the crystal lattice. A recent x-ray absorption spectroscopy (XAS) study of $\text{Ni}_c\text{Mg}_{1-c}\text{O}$ at the Ni K edge gives direct evidence for a shift of nickel ions upon dilution to the off-centre position, which is stimulated by the superexchange interaction and by the ionic radii difference of Ni^{2+} and Mg^{2+} ions [9]. The off-centre displacement of nickel ions is also supported by the results of the optical absorption and luminescence studies [10]. In contrast to the case for $\text{Ni}_c\text{Mg}_{1-c}\text{O}$, it is expected that cobalt ions in $\text{Co}_c\text{Mg}_{1-c}\text{O}$ should remain, upon dilution, at the regular lattice sites, being squeezed within the lattice due to a decrease of the lattice parameter a and the difference between the cobalt and magnesium ionic radii (the radius of the cobalt ion is about 0.02 \AA larger than that of the magnesium ion). This was confirmed by XAS, performed using a laboratory EXAFS spectrometer with a conventional x-ray tube [8]. Note that the new results on the Co K edge in $\text{Co}_c\text{Mg}_{1-c}\text{O}$, obtained by us using a more intense synchrotron radiation source and a more accurate analysis procedure, are consistent with previous observations,

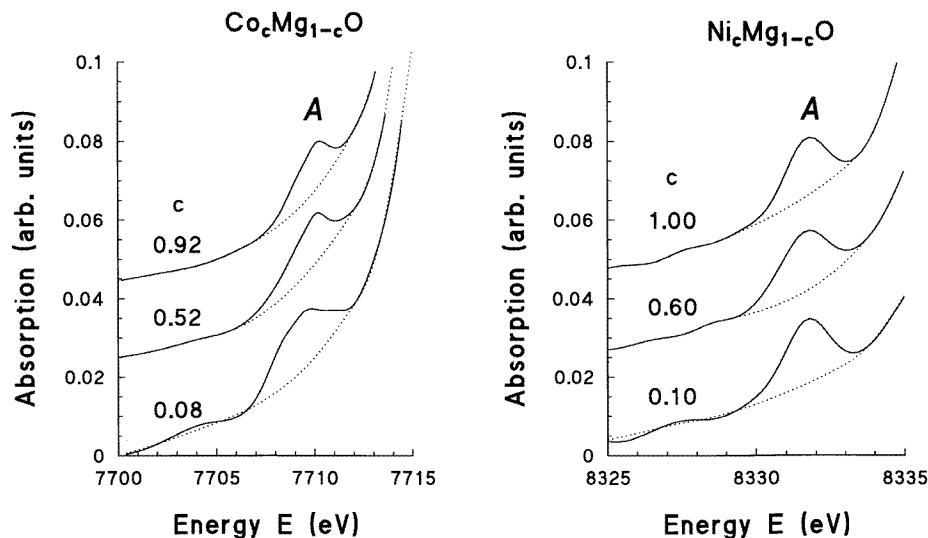


Figure 2. An expanded view of the pre-edge part of the Co and Ni K-edge XANES in $\text{Ni}_c\text{Mg}_{1-c}\text{O}$ and $\text{Co}_c\text{Mg}_{1-c}\text{O}$ solid solutions. The dotted lines are background approximations determined by a cubic spline fit to the data on either side of the pre-edge peak A. Only a few spectra are shown, for clarity.

and will be discussed further. Thus, the direct evidence obtained by means of XAS of the modifications, occurring within the local environment of TM ions, makes questionable the existing expectation of the constancy of J_{NN} - and J_{NNN} -interactions upon dilution [7].

In this work, we present a comparative analysis of the results on the local atomic environment, probed by means of extended x-ray absorption fine structure (EXAFS), and the local electronic structure, probed by means of x-ray absorption near-edge structure (XANES), around Co and Ni ions in $\text{Me}_c\text{Mg}_{1-c}\text{O}$ ($\text{Me} = \text{Co}, \text{Ni}$) solid solutions. In particular, we are going to discuss the influence of the $2\text{p}(\text{O})\text{-}3\text{d}(\text{Me})$ covalent mixing on the pre-edge peak intensity at the Co (Ni) K absorption edge, and its relationship with the magnetic properties of these solid solutions.

2. Experimental procedure and data analysis

The preparation of the solid solutions utilized in the present work was described by us previously [8, 9]. Briefly, the samples of $\text{Me}_c\text{Mg}_{1-c}\text{O}$ ($\text{Me} = \text{Co}, \text{Ni}$) were prepared by mixing the appropriate amounts of aqueous solutions of $\text{Mg}(\text{NO}_3)_2 \cdot 6\text{H}_2\text{O}$ and $\text{Me}(\text{NO}_3)_2 \cdot 6\text{H}_2\text{O}$ salts, which were slowly evaporated and heated up to $500\text{--}600^\circ\text{C}$ to remove the NO_2 completely. The polycrystalline solid solutions thus obtained were powdered, and annealed for 100 h at 1200°C in air, and then quickly cooled down to room temperature. The composition of the solid solutions was confirmed by instrumental neutron-activated analysis [17].

Experimental x-ray absorption spectra at the Co (Ni) K edge in $\text{Me}_c\text{Mg}_{1-c}\text{O}$ ($\text{Me} = \text{Co}, \text{Ni}$) solid solutions and the pure oxides MeO ($c = 1$) were measured at room temperature in the transmission mode at the ADONE storage ring (Frascati, Italy) on the PWA-BX2S wiggler beam line, equipped with a $\text{Si}(220)$ channel-cut crystal monochromator, and two

ion chambers containing krypton gas. The storage ring ADONE operated at the average energy 1.2 GeV and the maximum stored current 40 mA. The samples were prepared from finely ground $\text{Me}_c\text{Mg}_{1-c}\text{O}$ ($\text{Me} = \text{Co}, \text{Ni}$) powders, and had a thickness leading to the absorption jump $\Delta\mu x$ of about 0.5–2.0, depending on the composition. The normalized x-ray absorption near-edge structures (XANES) in solid solutions are shown in figure 1. Note that the two sets of XANES spectra are similar to each other, due to the closeness of the $\text{Me}_c\text{Mg}_{1-c}\text{O}$ ($\text{Me} = \text{Co}, \text{Ni}$) structures, and exhibit similar behaviour upon dilution (with the decrease of c).

Furthermore, we will be interested in the intensity variation of the pre-edge peak A, whose position is indicated in figure 1. The intensity of peak A, determined by its area, was obtained using the following procedure: the background contribution (dotted lines in figure 2) was approximated by a cubic spline fit to the data on either side of peak A, and subtracted from the normalized experimental XANES spectrum; the signal thus obtained was integrated over the range of the peak A.

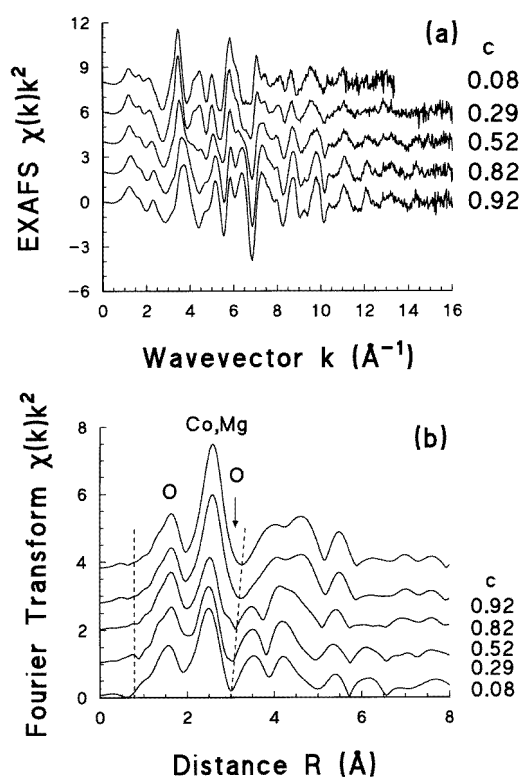


Figure 3. (a) Experimental EXAFS $\chi(k)k^2$ -spectra of $\text{Co}_c\text{Mg}_{1-c}\text{O}$. (b) Fourier transforms of the spectra shown in (a). Dashed lines indicate the range used in the analysis. Only a few spectra are shown, for clarity.

The EXAFS signals were treated using the EDA software package [18]. The results of the analysis for $\text{Ni}_c\text{Mg}_{1-c}\text{O}$ were reported in detail in [9]. The same procedure was applied to a set of the $\text{Co}_c\text{Mg}_{1-c}\text{O}$ data (figure 3). The variation upon dilution of the interatomic distances Co (Ni)–O, Co (Ni)–Co (Ni), and Co (Ni)–Mg obtained is shown in figure 4. Here we reproduce also the data for the $R(\text{Co}–\text{O})$ distance in the first shell obtained in [8].

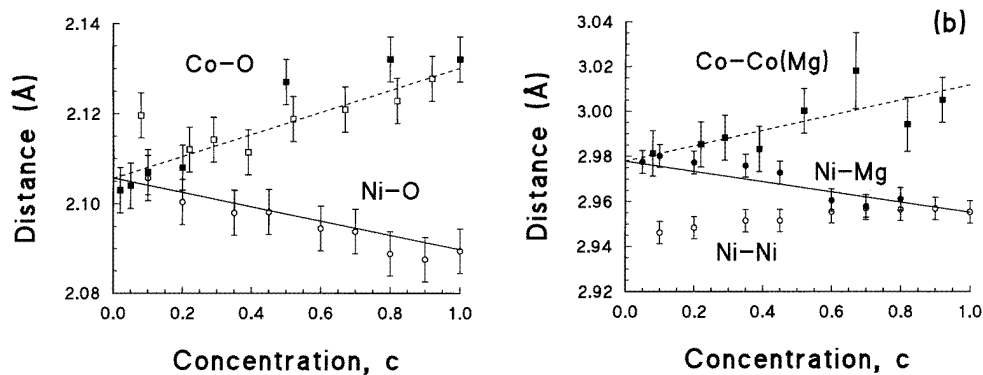


Figure 4. The variation of the average interatomic distances in $\text{Ni}_c\text{Mg}_{1-c}\text{O}$ and $\text{Co}_c\text{Mg}_{1-c}\text{O}$ with the composition: (a) $R(\text{Ni-O})$ (○) [9], $R(\text{Co-O})$ (□) (this work), and $R(\text{Co-O})$ (■) [8]; and (b) $R(\text{Co-Co(Mg)})$ (■) (this work), $R(\text{Ni-Ni})$ (○), and $R(\text{Ni-Mg})$ (●) [9]. The values of the interatomic distances, which were calculated in the virtual-crystal approximation (VCA) [19] from the average crystal lattice parameter given by XRD [2, 7], are also shown for comparison: (a) $R(\text{Co-O})$ (---) and $R(\text{Ni-O})$ (—); and (b) $R(\text{Co-Co(Mg)})$ (---) and $R(\text{Ni-Ni(Mg)})$ (—). Note that the distances $R(\text{Co-Co})$ and $R(\text{Co-Mg})$ in $\text{Co}_c\text{Mg}_{1-c}\text{O}$ were found to be equal, and to change upon dilution in agreement with the VCA model.

Note that the latter set of data is less accurate than the results of the present work, due to the fact that the experimental data used in [8] were recorded with smaller resolution, and also the analysis procedure utilized in [8] was less sophisticated. However, the results of [8] agree generally with the ones obtained in the present work.

3. Results and discussion

The XANES spectra in $\text{Me}_c\text{Mg}_{1-c}\text{O}$ ($\text{Me} = \text{Co}, \text{Ni}$) solid solutions are fairly similar, and vary upon dilution with decreasing c (figure 1). In particular, at small TM concentrations, the features at the edge become more pronounced, and change their positions slightly. Within the multiple-scattering approach, these effects were attributed by us to the substitution for the TM ions of magnesium ions, having scattering amplitudes and phase functions different from those of the TM ions, and to the change of the lattice parameter [9]. Note that the effect of the substitution dominates strongly over the change of the lattice constant, as directly follows from a comparison of the XANES in CoO and NiO , having the largest difference of the lattice parameters, with the XANES results for $\text{Co}(\text{Ni})_c\text{Mg}_{1-c}\text{O}$ solid solutions at small c (figure 1). However, a comparison of the XANES signals of the two solid solutions for close concentrations allows us to observe that, in spite of the general similarities, the broadening of the XANES at the Ni K edge is larger than at the Co K edge. This can be seen, for example, from a comparison of the features B, indicated in figure 1. It has been shown by the single-scattering [8, 9] and full-multiple-scattering [20] calculations that the feature B is mainly due to the photoelectron scattering by the eight oxygen atoms located in the third coordination shell of the Ni(Co) ion. The difference between the broadenings of the feature B in the two solid solutions leads us to suppose that it may be due to a static disorder which is present in the third shell of nickel. Such an interpretation is supported by the results from the EXAFS [9] and optical spectroscopies [10], suggesting that nickel ions shift upon dilution into off-centre positions, whereas cobalt ions remain at the centres of the CoO_6 octahedra. As a result of the Ni displacement, its third shell becomes split,

inducing the broadening of the feature B in XANES. The observed structural behaviour is directly related to the electronic and magnetic properties of the two solid solutions, which will be discussed below.

In our further considerations, we will concentrate our attention on the intensity variation of the pre-edge peak A, indicated in figure 1, and on its relationship with the change of the 2p(O)–3d(Me) (Me = Co, Ni) mixing, and magnetic interactions between the TM ions.

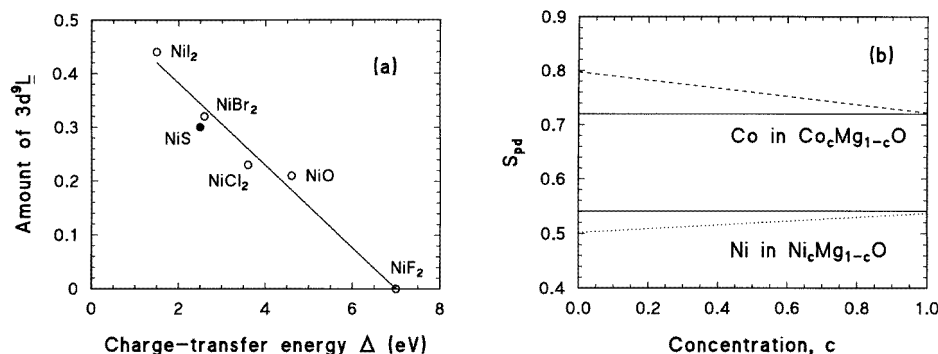


Figure 5. (a) The dependence of the amount of the 3d⁹L configuration on the value of the charge-transfer energy Δ in nickel compounds. The data shown by open circles are taken from [21]. The value for NiS is taken from [23]. (b) The estimated dependence of the 2p_σ(O)–3d(e_g)(Me) (Me = Ni, Co) overlap integral S_{pd} for different concentrations, assuming that the Ni(Co) ions are situated at the regular lattice site, i.e. they are not displaced to the off-centre positions ($R(\text{Me-O}) = (1/2)a$, where a is the lattice parameter).

NiO and CoO belong to a class of the charge-transfer insulators [12, 13] whose ground states (GS) are described within a framework of the Zaanen–Sawatzky–Allen (ZSA) model [12] as

$$\Psi_{\text{GS}}(\text{Ni}^{2+}) = a_0|3d^8\rangle + a_1|3d^9\bar{L}\rangle + a_2|3d^{10}\bar{L}^2\rangle \quad (1)$$

$$\Psi_{\text{GS}}(\text{Co}^{2+}) = a_0|3d^7\rangle + a_1|3d^8\bar{L}\rangle + a_2|3d^9\bar{L}^2\rangle + a_3|3d^{10}\bar{L}^3\rangle \quad (2)$$

where \bar{L} stands for an oxygen 2p hole. The amounts a_i ($i = 0, 1, 2$) of $|3d^{8+i}\bar{L}^i\rangle$ configurations in pure NiO were estimated recently in [21]: they are 0.73, 0.21, and 0.06, respectively, so only the first two configurations, corresponding to the pure ionic state without 2p holes and to the state with one electron transferred from an oxygen to a nickel ion, are significant. This conclusion is also consistent with the result obtained in [22] for LaNiO₃. In this compound, nickel ions have the valence state 3+, and their ground state is described as that of Co²⁺:

$$\Psi_{\text{GS}}(\text{Ni}^{3+}) = a_0|3d^7\rangle + a_1|3d^8\bar{L}\rangle + a_2|3d^9\bar{L}^2\rangle + a_3|3d^{10}\bar{L}^3\rangle. \quad (3)$$

The weights $a_0 = 0.6$ and $a_1 = 0.4$ were estimated in [22] for LaNiO₃. The situation, similar to that for NiO, should be observed in cobalt oxide, where it is anticipated that the $|3d^7\rangle$ and $|3d^8\bar{L}\rangle$ ground-state configurations have the largest weight. The quantities a_i in (1), (2), and (3) correlate strongly with the value of the charge-transfer energy Δ [21] (figure 5(a)), and, like Δ, are related to the value of the pd orbital mixing λ_{pd} , and to the covalency of the nickel–oxygen bond [21, 23]. Thus, Δ increases when the anion–cation pd covalent mixing λ_{pd} decreases, and the bonding becomes more ionic.

In the case of the Co (Ni) K-edge absorption, the transition of the 1s electron occurs from the core atomic state into a final unoccupied state that is the relaxed excited state in

the presence of the core hole at the 1s level screened by other electrons. In the dipole approximation, $\Delta l = \pm 1$ (l is the orbital momentum of the electron), the final state of the electron should have p character. Therefore, the pre-edge peak A can be attributed to the dipole-allowed transition $|\underline{1s}3d^{m+i}\underline{L}^i\rangle \rightarrow |\underline{1s}3d^{m+i}\underline{L}^{i-1}\rangle$ (here $\underline{1s}$ denotes a Ni(Co) 1s core hole; $i = 1, 2, 3$ and $m = 7$ for Co^{2+} ; $i = 1, 2$ and $m = 8$ for Ni^{2+}), into the final state (FS):

$$\Psi_{\text{FS}}(\text{Ni}^{2+}) = b_1|\underline{1s}3d^9L\rangle + b_2|\underline{1s}3d^{10}\underline{L}^1\rangle \quad (4)$$

$$\Psi_{\text{FS}}(\text{Co}^{2+}) = b_1|\underline{1s}3d^8L\rangle + b_2|\underline{1s}3d^9\underline{L}^1\rangle + b_3|\underline{1s}3d^{10}\underline{L}^2\rangle. \quad (5)$$

In the sudden approximation [24], the intensity of the pre-edge peak A is given by $|a_1b_1 + a_2b_2|^2$ for NiO and $|a_1b_1 + a_2b_2 + a_3b_3|^2$ for CoO. Finally, one should note that both ground, Ψ_{GS} , and final, Ψ_{FS} , states are characterized by a strong mixing of the oxygen 2p and nickel/cobalt 3d orbitals.

The interpretation of the origin of the pre-edge peak A given above is strongly supported by self-consistent-field (SCF) multiple-scattering (MS) calculations performed for the Ni K edge in $\text{La}_{1-x}\text{Nd}_x\text{NiO}_3$ and $\text{LaNi}_{1-x}\text{Fe}_x\text{O}_3$ perovskites [22]. In these materials the ground-state configuration of nickel ions is described by (3), with three states, $|3d^8\underline{L}\rangle$, $|3d^9\underline{L}^2\rangle$, and $|3d^{10}\underline{L}^3\rangle$, being dipole allowed for the transition of the 1s(Ni) electron which is observed as the pre-edge peak. In [22], only two configurations, $|3d^7\rangle$ and $|3d^8\underline{L}\rangle$, were considered in the calculations. The results obtained show that the intensity of the pre-edge peak A correlates strongly with the amount of the $|3d^8\underline{L}\rangle$ configuration in the ground state [22]. Therefore, one can use the intensity of the pre-edge peak A as an estimate of the pd mixing λ_{pd} [21]. The value of λ_{pd} is proportional to the overlap between 3d TM and 2p O orbitals, whose variation in solid solutions can be estimated. To do this, we consider a simple model described below.

The empty final state, probed by the Co (Ni) K-edge absorption, has $2p_\sigma(\text{O})-3d(e_g)(\text{Me})$ ($\text{Me} = \text{Co}, \text{Ni}$) character (the $3d(t_{2g})$ sub-band is filled both in CoO and NiO); therefore, to estimate roughly the change of the pd mixing upon dilution, we evaluated the $\langle 2p_\sigma(\text{O})|3d(e_g)(\text{Me})\rangle$ ($\text{Me} = \text{Co}, \text{Ni}$) overlap integral using simple Slater-type (exponential) nodeless atomic orbitals [25]:

$$\begin{aligned} \chi_{nlm}(r, \zeta) &= R_{nl}(r, \zeta)Y_{lm}(\theta, \phi) \\ R_{nl}(r, \zeta) &= C_n(r/a_0)^{n^*-1} \exp(-\zeta r/a_0) \quad C_n = (2\zeta)^{(n^*+1)/2}/[(2n)!]^{1/2} \end{aligned} \quad (6)$$

where Y_{lm} is a normalized spherical harmonic; C_n is the normalization constant of the radial component R_{nl} ; a_0 is the first Bohr hydrogen radius; $\zeta = (Z - \gamma)/n^*$ is the exponent parameter; n^* is the effective main quantum number; γ is the screening constant; and $Z - \gamma$ is the effective charge.

The parameters ζ and n^* , used in the calculation, were chosen according to the procedure described in [25]. Their values are $\zeta(\text{Co}^{2+}) = 6.9$, $\zeta(\text{Ni}^{2+}) = 7.55$, $\zeta(\text{O}^{2-}) = 2.275$, $n^*(\text{Co}^{2+}) = n^*(\text{Ni}^{2+}) = 3$, and $n^*(\text{O}^{2-}) = 2$. The $\text{Co}^{2+}(\text{Ni}^{2+})$ and O^{2-} ions were placed along the z -axis at the distance r_0 from one another. The distance r_0 between the TM (Co or Ni) and oxygen ions was varied over the range observed for the respective solid solutions: from 2.106 to 2.130 Å in $\text{Co}_c\text{Mg}_{1-c}\text{O}$ and from 2.106 down to 2.090 Å in $\text{Ni}_c\text{Mg}_{1-c}\text{O}$. The angular orbital components Y_{lm} were taken for the d_{z^2} orbital in the case of the TM ion, and for the p_z orbital in the case of the oxygen ion. The overlap integral $S_{pd} = \langle \chi_{nlm}(r, \zeta)(\text{Co}(\text{Ni})) | \chi_{nlm}(r + r_0, \zeta)(\text{O}) \rangle$ was evaluated numerically.

The results obtained show a linear dependence of S_{pd} on the interatomic distance. Therefore, if one assumes in the case of solid solutions that the Ni(Co) ions are situated at the regular lattice sites ($R(\text{Ni}(\text{Co})-\text{O}) = (1/2)a$, where a is the lattice parameter), then it is expected that the overlap integral S_{pd} will change linearly with the composition (figure 5(b)).

Besides this, upon dilution, the S_{pd} -value should increase by $\sim 10\%$ in $\text{Co}_c\text{Mg}_{1-c}\text{O}$ and decrease by $\sim 7\%$ in $\text{Ni}_c\text{Mg}_{1-c}\text{O}$; such behaviour of S_{pd} reflects an expansion and a contraction of the crystal lattice in solid solutions, leading to a decrease/increase of the pd overlap. However, the results of the EXAFS analysis show that the above assumption holds true only in the $\text{Co}_c\text{Mg}_{1-c}\text{O}$ system, in which, upon dilution, cobalt ions remain at the regular lattice sites, being squeezed within the crystal lattice, and the average cobalt–cobalt distance decreases along with the lattice parameter. In contrast, nickel ions in $\text{Ni}_c\text{Mg}_{1-c}\text{O}$ shift upon dilution to the off-centre position, so the average nickel–nickel distance remains nearly constant (figure 4(b)) [9, 10]. Note that static distortion of the first coordination shell around nickel ions is not observed (figure 4(a)), because its value ($\sigma_{\text{st}}^2 \approx 0.0012 \text{ \AA}^2$) is smaller than the one ($\sigma_{\text{th}}^2 \approx 0.0038 \text{ \AA}^2$ (see the data given in table 1 for pure NiO in [9])) due to the thermal disorder. Thus, only a small variation of the overlap integral S_{pd} , and thus of the pd mixing, can be expected in $\text{Ni}_c\text{Mg}_{1-c}\text{O}$, owing to the distortion of the local environment. As we will see below, these results are in good agreement with the observed pre-edge peak intensity, related to the value of the pd mixing, λ_{pd} .

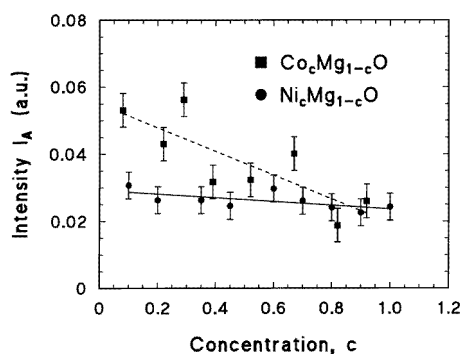


Figure 6. The variation of the intensity I_A of the pre-edge peak A with the concentration. The solid and dashed lines show linear approximations for $\text{Ni}_c\text{Mg}_{1-c}\text{O}$ and $\text{Co}_c\text{Mg}_{1-c}\text{O}$, respectively. The error bars are mainly due to the inaccuracies in the background (dotted lines in figure 2) subtraction procedure used to isolate the pre-edge peak.

The variation of the pre-edge peak intensity I_A in solid solutions is shown in figure 6. The linear least-squares fits suggest that, upon dilution, I_A increases by a factor of about 1.2 in $\text{Ni}_c\text{Mg}_{1-c}\text{O}$, whereas it grows by a factor of about 2.8 in $\text{Co}_c\text{Mg}_{1-c}\text{O}$. This means that, upon dilution, the weight of the $|3d^{n+i}\underline{L}^i\rangle$ ($i > 0$) ground-state configurations increases, due to an increase of the charge transfer from oxygen ligands to TM ions, and the effect is much stronger in the $\text{Co}_c\text{Mg}_{1-c}\text{O}$ system than in $\text{Ni}_c\text{Mg}_{1-c}\text{O}$. In fact, this suggests the lowering of the charge-transfer energy Δ , and an increase of the pd mixing λ_{pd} (as well as S_{pd}). A comparison of the experimentally determined dependences of I_A (figure 6) with the calculated variations of S_{pd} (figure 5(b)) versus c allows us to conclude that they behave similarly in the case of $\text{Co}_c\text{Mg}_{1-c}\text{O}$ solid solutions, supporting the absence of the off-centre displacement of Co^{2+} ions found from EXAFS data. On the other hand, for $\text{Ni}_c\text{Mg}_{1-c}\text{O}$ solid solutions, I_A increases slightly upon dilution, while the model based on the central position of Ni^{2+} ions suggests a decrease of S_{pd} and thus of I_A . This contradiction can be understood by taking into account the results of the EXAFS [9] and optical spectroscopies [10]: they show that Ni^{2+} ions shift into the off-centre position upon dilution, so the Ni–Ni distance remains nearly unchanged. This effect was explained in [9, 10] by the presence

of $\text{Ni}^{2+}-\text{O}^{2-}-\text{Ni}^{2+}$ ($\widehat{\text{NiONi}} = 90^\circ$) superexchange interactions, which persist also for low concentrations of nickel ions. Thus, an increase of I_A for $\text{Ni}_c\text{Mg}_{1-c}\text{O}$ correlates with the off-centre displacement of Ni^{2+} ions, and suggests also a possible change of the 90° superexchange interaction due to a slightly larger overlap of nickel d and oxygen p orbitals.

Now the following question arises. What is the influence of the 2p–3d mixing on the magnetic properties of solid solutions? In particular, how does it correlate with the concentration dependence of the Néel temperature?

Recent theoretical calculations show that the pd mixing plays only a minor role with respect to the magnetic and insulating properties of pure CoO and NiO [26]. However, it is known [27] that the change of λ_{pd} should affect the strength of the superexchange interactions J : for example, the cation–anion–cation interaction $J_{\text{NNN}}(180^\circ) \propto \lambda_{pd}^4$ [27]. Therefore, from the variation of the pre-edge peak intensity (figure 6), it is expected that, upon dilution, both superexchange parameters, J_{NN} and J_{NNN} , will increase in $\text{Co}_c\text{Mg}_{1-c}\text{O}$, whereas they will remain nearly constant or increase slightly in $\text{Ni}_c\text{Mg}_{1-c}\text{O}$. At the same time, the concentration dependences of the Néel temperature $T_N(c)$ (see figure 1 in [11]) are rather similar for the two solid solutions: T_N decreases upon dilution, in good agreement with the molecular-field approximation (MFA) at $c > 0.6$, where its dependence on c is linear (note that in the MFA [11] $T_N(c) = S(S+1)|J_{\text{NNN}}|z_{\text{NNN}}c/(3k_B)$, where S is the total spin moment, z_{NNN} is the number of next-nearest-neighbour metal ions involved in the superexchange interaction, and k_B is the Boltzmann constant). Since the Néel temperature is proportional (within the MFA) to the superexchange parameter, the expected increase of J upon dilution, and the difference between the values of J for the two solid solutions are in seeming contradiction with the similarity of their magnetic phase diagrams [11]. This problem can be resolved if one considers the contribution of the nearest-neighbour superexchange interaction, J_{NN} . In the pure NiO (CoO) system, the J_{NN} -contribution to T_N is not present due to the equal number (six) of nearest neighbours having spins oriented parallel and antiparallel, causing their total molecular field at a given ion to be cancelled out. The role of the nearest-neighbour interactions, J_{NN} , should increase upon dilution, which can be related to the observed deviation of $T_N(c)$ from the linear MFA behaviour at $c < 0.6$ [11]. Therefore, the difference in the expected variation of J for two solid solutions, while their magnetic phase diagrams are similar, allows us to assume that their magnetic properties are determined by the ratio $J_{\text{NNN}}/J_{\text{NN}}$. A similar conclusion has been reached recently in [7] by comparing the magnetic phase diagrams of $\text{Me}_c\text{Mg}_{1-c}\text{O}$ ($\text{Me} = \text{Co}, \text{Ni}$) with those of $\text{Eu}_c\text{Sr}_{1-c}\text{S}$ and $\text{Eu}_c\text{Sr}_{1-c}\text{Te}$.

4. Summary and conclusions

In this work, the influence of the 2p(O)–3d(Me) ($\text{Me} = \text{Co}, \text{Ni}$) mixing and magnetic interactions on the pre-edge peak intensity at the Co (Ni) K absorption edge in $\text{Me}_c\text{Mg}_{1-c}\text{O}$ solid solutions is discussed.

The systems considered are related to a class of the charge-transfer isolators, so the origin of the pre-edge peak is attributed to the amount of $|3d^{n+i}\underline{L}^i\rangle$ ($i > 0$) ground-state configurations with oxygen 2p hole(s). It is observed that the intensity of the pre-edge peak grows upon dilution by a factor of 1.2 in $\text{Ni}_c\text{Mg}_{1-c}\text{O}$ and by a factor of about 2.8 in $\text{Co}_c\text{Mg}_{1-c}\text{O}$. This fact is explained by an increase of the p(O)–d(Me) ($\text{Me} = \text{Co}, \text{Ni}$) overlap S_{pd} , leading to an increase of the pd-mixing value, λ_{pd} , and, thus, the strength of the superexchange interactions, J . The results obtained are in agreement with the modifications of the local atomic structure around the Co^{2+} and Ni^{2+} ions probed by EXAFS [8, 9] and

optical spectroscopies [10].

It is expected that the variation of J with the composition is different for the two solid solutions, while their magnetic phase diagrams are rather similar [11], and are characterized by a deviation for $c < 0.6$ of the concentration dependence of the Néel temperature from the linear behaviour suggested within the molecular-field approximation [11]. These facts lead us to propose that the important quantity in diluted solid solutions is the ratio of the superexchange parameters, $J_{\text{NNN}}/J_{\text{NN}}$.

Acknowledgments

JP wishes to thank Professor E Burattini (Laboratori Nazionali di Frascati) and the staff of the PWA laboratory for providing us with the possibility of making measurements at the PWA-BX2S beam line.

References

- [1] Archipov A A 1981 *Izv. Akad. Nauk Latv. SSR, Ser. Fiz. Tech. Nauk* **3** 24
- [2] Kannan R and Seehra M S 1987 *Phys. Rev. B* **35** 6847
- [3] Seehra M S and Giebultowicz T M 1988 *Phys. Rev. B* **38** 11 898
- [4] Giebultowicz T M, Rhyne J J, Seehra M S and Kannan R 1988 *J. Physique Coll.* **49** C8 1105
- [5] Asakura K and Iwasawa Y 1988 *Mater. Chem. Phys.* **18** 499
- [6] Menshikov A Z, Dorofeev Yu A, Klimenko A G and Mironova N A 1991 *Phys. Status Solidi b* **164** 275
Menshikov A Z, Dorofeev Yu A, Klimenko A G and Mironova N A 1990 *Zh. Eksp. Teor. Fiz. Pis.* **51** 640
- [7] Feng Z and Seehra M S 1992 *Phys. Rev. B* **45** 2184
- [8] Kuzmin A, Mironova N, Purans J and Sazonov A 1993 *Phys. Status Solidi a* **135** 133
Kuzmin A, Mironova N, Purans J and Sazonov A 1993 *Japan. J. Appl. Phys. Suppl.* **2** **32** 637
- [9] Kuzmin A, Mironova N, Purans J and Rodionov A 1995 *J. Phys.: Condens. Matter* **7** 9357
- [10] Mironova N, Kuzmin A, Purans J and Rodionov A 1995 *Proc. SPIE* **2706** 168
- [11] Menshikov A Z, Dorofeev Yu A, Mironova N A and Medvedev M V 1996 *Solid State Commun.* **98** 839
- [12] Zaanen J, Sawatzky G A and Allen J W 1985 *Phys. Rev. Lett.* **55** 418
Zaanen J and Sawatzky G A 1987 *Can. J. Phys.* **65** 1262
- [13] Shen Z X, Allen J W, Lindberg P A P, Dessau D S, Wells B O, Borg A, Ellis W, Kang J S, Oh S J, Lindau I and Spicer W E 1990 *Phys. Rev. B* **42** 1817
- [14] Kübler J and Williams A R 1986 *J. Magn. Magn. Mater.* **54–57** 603
- [15] ter Haar D and Lines M E 1962 *Phil. Trans. R. Soc. A* **254** 521
- [16] van Vleck J H 1941 *J. Chem. Phys.* **9** 85
- [17] Mironova N A and Ulmanis U A 1988 *Radiation Defects and Metal Ions of the Iron Group in Oxides* (Riga: Zinatne) (in Russian)
- [18] Kuzmin A 1995 *Physica B* **208+209** 175
Kuzmin A 1996 *EDA: EXAFS Data Analysis Software Package Users Manual* (available from the author)
Kuzmin A 1997 *J. Physique IV* at press
- [19] Letardi A, Motta N and Balzarotti A 1987 *J. Phys. C: Solid State Phys.* **20** 2853
- [20] Kizler P 1992 *Phys. Rev. B* **46** 10 540
- [21] van der Laan G, Zaanen J, Sawatzky G A, Karnatak R and Esteve J M 1986 *Phys. Rev. B* **33** 4253
van Veenendaal M A and Sawatzky G A 1994 *Phys. Rev. B* **50** 11 326
- [22] Garcia J, Blasco J, Proietti M G and Benfatto M 1995 *Phys. Rev. B* **52** 15 823
- [23] Bocquet A E, Mizokawa T, Fujimori A, Matoba M and Anzai S 1995 *Phys. Rev. B* **52** 13 838
- [24] Mizokawa T, Fujimori A, Arima T, Tokura Y, Mōri N and Akimitsu J 1995 *Phys. Rev. B* **52** 13 865
- [25] Bersuker I B 1976 *Electronic Structure and Properties of Coordination Compounds* (Leningrad: Khimia) (in Russian)
- [26] Nolting W, Haunert L and Borstel G 1992 *Phys. Rev. B* **46** 4426
- [27] Goodenough J B 1971 *Prog. Solid State Chem.* **5** 145